University Library

A gateway to Melbourne's research publications

Minerva Access is the Institutional Repository of The University of Melbourne

Author/s:
Sharma, A;Singh, MB;Bhalla, PL

Title:
Cytochemistry of pollen development in Brachypodium distachyon

Date:
2014-01-01

Citation:
Sharma, A., Singh, M. B. & Bhalla, P. L. (2014). Cytochemistry of pollen development in Brachypodium distachyon. Plant Systematics and Evolution, 300 (7), pp.1639-1648. https://doi.org/10.1007/s00606-014-0989-9.

Persistent Link:
https://hdl.handle.net/11343/283173

Cytochemistry of pollen development in *Brachypodium distachyon*

Akanksha Sharma, Mohan B Singh and Prem L Bhalla[§]

Plant Molecular Biology and Biotechnology Laboratory, Australian Research Council Centre of Excellence for Integrative Legume Research, Melbourne School of Land and Environment, University of Melbourne, Parkville, Victoria 3010, Australia

[§]Corresponding Author

Telephone number: +613 83449651

Email address: premlb@unimelb.edu.au

Abstract

Brachypodium distachyon is a widely recognized model plant belonging to subfamily Pooideae with a sequenced genome. To gain a better understanding of the male reproductive development in *B. distachyon*, we examined pollen morphology and cytochemical changes of microspore cytoplasm from pollen mother cell stage to mature pollen using light, fluorescent and scanning electron microscopy. Our results show that *B. distachyon* exhibits a typical monocot-type pollen ontogeny. Meiosis in the pollen mother cells is accomplished by successive cytokinesis generating isobilateral tetrads. Cytochemical examination indicated that microspore cytoplasm contains variable amounts of insoluble carbohydrates and proteins at different developmental stages. Deposition of starch in the cytoplasm of microspores starts at the bicellular stage and continues till the mature pollen stage. The formation of the exine wall progresses by the deposition of sporopollenin from the tapetum layer of the anther. The mature pollen is trinucleate, spheroidal in shape and possesses a single pore with an annulus and operculum. The exine pattern is smooth and of granular type.

Keywords *Brachypodium*, pollen, pollen development, male gametophyte, cytochemistry

Introduction

Brachypodium distachyon has been recognized as an ideal model plant for grass functional genomics as it is phylogenetically related to important food crops and turf grasses. The availability of the genome sequence and protocols for the plant transformation allows investigations of the functional role of genes in this plant. It is a small, easy-to-cultivate and a rapidly growing grass, native of North Africa, South Europe, and Central Asia. It is a self-pollinated plant reaching up to 15–20 cm height at maturity and has a short life cycle (8-12 weeks) (Draper et al. 2001; Garvin et al. 2008; Opanowicz et al. 2008; Vogel and Hill 2008; International Brachypodium Initiative, 2010; Vain 2011). Among grasses, it exhibits one of the smallest genomes (272 Mbp; 26,000 genes) (Alves et al. 2009). Hence, *B. distachyon* has the potential to become the grass equivalent of *Arabidopsis* for research purposes.

The transitional location of *B. distachyon* linking the *Triticeae* (wheat) and the *Ehrhartoideae* (rice) makes it a perfect model to carry out comparative studies and tracing back the evolutionary relationships in these plants. To date, the basic information regarding structural and cytological development of the male gametophyte in *B. distachyon* is lacking. Several reports published on anther and pollen development of Poaceae members such as wheat (Goss 1968; Saini et al. 1984; El-Ghazaly and Jensen 1986; Mizelle et al. 1989), rice (Raghavan 1988; Itoh et al. 2005; Zhang and Wilson 2009; Zhang et al. 2011), rye (Heslop-Harrison 1979), sorghum (Christensen et al. 1972), maize (Skvarla and Larson 1966), barley (Charzynska and Lenart 1989) and ryegrass (Vithanage and Knox 1980) contribute to our understanding of the male reproductive process in this grass family. Hence, it would be interesting to compare *B. distachyon* pollen development with other well-studied monocots (wheat and rice) to characterize discrete developmental stages in *B. distachyon*. Our study addresses the ontogeny and cytochemistry of pollen in *B. distachyon* that would contribute towards our understanding of the reproductive biology of this model plant.

Pollen grain development is of pivotal significance in sexual reproduction of flowering plants. The role of the pollen grain is to produce and deliver male gametes (sperm cells) to the embryo sac, resulting in the successful fertilization of egg and eventually seed set. The process of pollen development takes place in the anther and comprises a sequence of events involving microspores and pollen grains undergoing remarkable structural changes. Anther and pollen developmental studies not only provide valuable information about their structure

and function but also contribute towards our understanding of taxonomic and evolutionary relationships in flowering plants (Chen et al. 2012).

The mature pollen grains act as a storage site for reserve substances such as lipids, carbohydrates and proteins which are essential for the initiation and growth of the pollen tube (Rodriguez-Garcia et al. 2003). For example, lipids are important as energy reserves for the development and functioning of pollen grains. However, the quantity and distribution of these reserve substances vary according to the stages of pollen maturation. The amount and nature of storage substances and the architecture of pollen wall also differ among species of flowering plants. (Eliseu and Dinis 2008).

The present study was undertaken to identify different stages of pollen development in *B. distachyon* and to provide related descriptions of accompanying cytological and anatomical characteristics. In addition, this study aimed to detect the distribution of reserve substances such as insoluble polysaccharides, proteins through the sequential pollen developmental stages in *B. distachyon*.

Materials and methods

B. distachyon (Bd21-3) plants (Fig. 1) were grown in the glasshouse under the controlled conditions as described by Vogel and Hill (2008). Since a description of the growth stages in *B. distachyon* is already available (Hong et al. 2011), the development of the spikelet was observed closely from the end of the booting stage, when the first awn was just visible out of the flag leaf (Fig. 1b), until mature anthers (Fig. 1e) were seen. With the onset of the first awn, the spikelet was selected as the ‘day 1’ spikelet. The spikelets were subsequently collected on successive days from day 1 until anthesis, a period of 9 days. Immature spikelets were dissected with the awns removed (1 to 5 days) and the anthers were excised from the base florets of mature spikelets (6 to 9 days). The entire protocol was conducted in three replicates.

Light microscopy

For light microscopy studies, spikelets and anthers were fixed immediately in cold 2.5% glutaraldehyde/0.1 M PBS (phosphate-buffered saline), at pH 7.0 for 4 h at room temperature. After two washes of 30 min each with PBS buffer, the spikelets and anthers were dehydrated in a series of increasing concentrations of ethanol in water (30%, 50%, 70%, 80%, 90%) for 1 h each and finally in 100% ethanol, rotating overnight. Spikelets and anthers were then incubated in 1:1 and 1:3 ethanol: resin (LR White) mixtures for 1 day each at room temperature and finally in 100% resin, rotating overnight. Following dehydration, spikelets and anthers were embedded in LR White, polymerized by incubation at 60˚for 24-30 h and sliced to 0.5 µm thickness with a Leica Ultracut® microtome.

For cytochemical examination, semithin sections were stained with periodic acid-Schiff (PAS) reagent and iodine-potassium iodide (I_2-KI) for detecting insoluble carbohydrates such as starch, with coomassie brilliant blue for detecting proteins, with DAPI (4',6-diamino-2-phenylindole) for detecting DNA, and with toluidine blue for detecting acidic polyanions, pectin and lignin. For PAS and coomassie brilliant blue staining, the methodology given by Tütüncü Konyar and Dane (2012) was slightly modified and adapted to the LR White resin-embedded sections.

Periodic-acid-Schiff (PAS) reaction for insoluble carbohydrates

Semithin sections were first oxidized in 1% periodic acid for 2 h, left in 90% alcohol for 5 min and washed in distilled water. The sections were then stained with Schiff's reagent for 1 h at room temperature, rinsed briefly in distilled water, destained three times with 0.5% sodium bisulfite for 2 min each, and again washed for 5 min in distilled water. Insoluble polysaccharides were stained pink to purple.

Coomassie brilliant blue for proteins

0.3% Coomassie brilliant blue staining solution (45% methanol, 10% glacial acetic acid, 45% water and 0.3 g Coomassie brilliant blue dye) was used to stain semithin sections of *B. distachyon* spikelets and anthers. The sections were stained for 90 min at room temperature, and then rinsed in distilled water. Proteins were stained blue.

Toluidine blue for acidic polyanions, pectin and lignin

Semithin sections were stained in 1% toluidine blue at room temperature for 10 min and rinsed in distilled water for 2 min. Toluidine blue stains acidic polyanionic groups (polyphosphates of nucleic acids), blue; lignin and phenol compounds, green; acidic polysaccharides like pectic acid, red or purple metachromasia (Halac et al. 2003; Pigman 2012; Tütüncü Konyar and Dane 2012; Tütüncü Konyar and Dane 2013b).

Iodine-Potassium iodide (I_2-KI) for starch

Semithin sections were stained with I_2-KI staining solution (10% Potassium iodide and 5% iodine crystals). The sections were stained for 10 min at room temperature and rinsed with distilled water. Starch granules were stained blue-black.

DAPI (4', 6-diamidino-2-phenylindole) for DNA (Fluorescent microscopy)

Staining solution was prepared by adding 0.5 µl DAPI (0.1 mg/ml) in 1 ml PBS (pH 7.0). Semithin sections of spikelets and anthers were stained for 4-6 h at room temperature in dark to achieve successful staining results. DAPI fluorescence was detected with an excitation light of 365 nm.

Scanning Microscopy

The mature anthers were fixed in 2.5% gluteraldehyde/0.1 M PBS (phosphate-buffered saline), pH 7.0, dehydrated in a graded ethanol series and critical point dried. Then, the anthers were mounted on aluminium stubs, tweezed to release pollen, sputter-coated with gold and photographed using Philips XL30 Field-emission Scanning electron microscope.

Results

In *B. distachyon*, each mature spike contains a number of spikelets, each of which in turn bears from two to nine flowers, known as florets. With the emergence of the first awn, at day 1 (Fig. 1b) until day 5, immature spikelets were fixed and sectioned. These sections each showed more than one anther event, and hence, more than one stage of development was identified in the same section. In these sections, the most developed stage was found in the base floret. For instance, if the microspores of the base floret were at the free microspore stage, the second from base floret would be at the tetrad stage, and the third from base floret would be at the pollen mother cell stage. At 6 to 9 days, anthers were harvested from the base floret of the spikelets, sectioned and single stages of development were identified (Table 1). The immature anthers of *B. distachyon* were green in color and attached to short filaments, whereas the mature anthers appeared yellow (Fig. 1e) and were attached to elongated filaments.

The results of pollen cytology are divided into sections based on the following major discrete stages of pollen ontogeny: Pollen mother cell, tetrad, free microspore, vacuolated microspore, bicellular pollen grain and mature pollen grain. The related description of major events corresponding to these stages was described in Table 2.

Pollen mother cell stage

This is the first stage in the course of pollen development. Pollen mother cells (PMCs), also called microspore mother cells, (MMCs) develop from the mitotic divisions of sporogenous cells. These cells were large in size and possessed a single nucleus of relatively large volume (Fig. 2a). PMCs were surrounded by a callose wall that separated them from the tapetum. Cytochemical staining showed that PMCs contained acidic polyanions (Fig. 2b) and proteins (Fig. 2c) in their cytoplasm. However, PMCs did not show any evidence of the presence of insoluble polysaccharides (starch) in their cytoplasm (Fig. 2d).

Tetrad stage

In *B. distachyon*, pollen mother cells underwent meiosis, forming dyads and eventually isobilateral tetrads (Fig. 3a, b) that were surrounded by a thick callose wall. Cytochemical tests showed that the microspores in the tetrad stage gave positive staining for the presence of acidic polyanions (polyphosphates of nucleic acids) (Fig. 3b). Intense Coomassie brilliant blue staining revealed staining for proteins (Fig. 3c). The tetrad microspores have dense cytoplasm and evident nuclei in the central region (Fig. 3d). At this stage, microspores did not show presence of insoluble polysaccharides such as starch in their cytoplasm (Fig. 3e) as evident by absence of PAS staining.

Free microspore stage

After meiosis, the callose wall surrounding the tetrads was degraded by the enzyme callase secreted from the tapetal cells and free haploid microspores were released. The just-released microspores were almost spherical (Fig. 3f), have thin exines and contained a centrally-located nucleus in their cytoplasm (Fig. 3f).

Vacuolated microspore stage

As the development progressed towards vacuolation, the microspore nucleus migrated to the periphery of the cell (Fig. 4a). At the beginning of this stage, the microspores have an irregular contour and are in contact with the tapetum. They showed the formation of exine layers by the addition of sporopollenin from the tapetum and the development of a single pore oriented towards the tapetum (Fig. 4b). Soon, the microspores increased in volume and became spherical with the formation of a large central vacuole (Fig. 4b). At the vacuolated microspore stage, low level of staining for acidic polyanions (Fig. 4b) and proteins (Fig. 4c) was observed. Starch accumulation has not occurred till this stage of development (Fig. 4d, e).

Bicellular pollen grain

Following vacuolation, the pollen nucleus undergoes first mitotic division (asymmetric cell division), generating a much smaller generative cell and a larger vegetative cell (Fig. 5a). At this stage it was observed that pollen grains started accumulating starch in their cytoplasm (Fig. 5b, c). Proteins (Fig. 5d) and acidic polyanions (Fig. 5e) were also detected in the cytoplasm of the pollen. Due to the accumulation of starch, the vacuole started diminishing gradually and the generative cell moved closer to the vegetative nucleus. Bicellular pollen grains were characterized by the presence of well-defined pollen walls.

Mature pollen grain

In *B. distachyon*, the mature pollen grain was oval in shape and trinucleate containing a vegetative nucleus and two sperm cells, formed by mitotic division of generative cell. (Fig.6a). It was observed that most of the cytoplasm of mature pollen contained starch grains (Fig. 6b, c). Proteins (Fig. 6d) and acidic polyanions (Fig. 6e) were also detected in the cytoplasm of the pollen grain.

Pollen morphology

Morphological analysis showed that mature pollen grain of *B. distachyon* was spheroidal in shape and contained a single operculate-annulate pore (Fig. 7). The exine was smooth and uniform with granular ornamentation (Fig. 7e, f).

Discussion

Our study provides the first report on the cytochemistry of pollen development in *B. distachyon*. The pattern of pollen ontogeny in *B. distachyon* is similar to other monocots in general as well as to other members of the Poaceae such as wheat (Goss 1968; Saini et al. 1984; Mizelle et al. 1989), rice (Raghavan 1988; Itoh et al. 2005; Zhang and Wilson 2009; Zhang et al. 2011), maize (Skvarla and Larson 1966), ryegrass (Vithanage and Knox 1980).

In rice, allometric relationships have been established between the growth of florets, anthers and pollen development (Raghavan, 1988). In wheat, plants were selected at the PMCs meiosis stage and anthers were harvested between meiosis and anthesis on successive days, for a period of 9 or 10 days (Saini et al. 1984). In this report, we have assigned ten stages of anther and pollen development occurring over a period of nine days of spikelet development after the first awn was visible as described in Table 1. Further, we investigated cytochemical changes taking place in the developing microspores of *B. distachyon* from pollen mother cell to mature pollen stage.

The microspore mother cells (MMCs) divide meiotically to produce microspore tetrads. Cytokinesis occurs after each meiotic division (successive type) and thus the isobilateral tetrad of microspores is formed. Similar results have been reported in rice (Zhang et al. 2011) and wheat (El-Ghazaly and Jensen 1986; Mizelle et al. 1989). The haploid microspores remain enclosed in the callose wall during the tetrad stage. An important function of the tapetal cell is the production and secretion of the enzyme β-1, 3-glucanase, or callase which break down the callose wall (Steiglitz, 1977). The young, just-released microspores have thin walls (Fig. 3f). The vacuolated microspores were irregularly shaped and in contact with the tapetum (Fig. 4). Similar irregular shaped microspores at the vacuolated stage have been reported in wheat (Saini et al. 1984). During vacuolated microspore stage, the single microspore pore (aperture) was observed, always oriented towards the tapetum and a close contact between the pore and tapetum was maintained (Fig. 4b). Similar observations have been reported in wheat (Saini et al. 1984), barley (Charzynska and Lenart 1989) and ryegrass (Vithanage and Knox 1980) where pollen aperture lies adjacent to the tapetal surface. However, from the literature it is evident that, during the late tetrad period, as the primexine (exine precursor) continues to thicken, the pore sites become apparent (Heslop-Harrison, 1963).

In vacuolated microspores, the exine showed the same staining reaction with the Orbicules/Ubisch bodies found on the inner surface of the tapetum (Fig. 4b). Ubisch bodies (Orbicules) are corpuscles of sporopollenin coating the inner tangential surface of tapetal cells (Heslop-Harrison and Dickinson 1969, Hesse 1986). Thus, it was revealed that sporopollenin, which was added to the exine, originated from the tapetum. Our results support the study in rice by Zhang et al. (2011), where they reported that the rice tapetum produce characteristic Orbicules/Ubisch bodies that export sporopollenin precursors to the

locule. In wheat, El-Ghazaly and Jensen (1986) reported that Pre-Ubisch bodies that are produced in the tapetal cells formed the core of the Ubisch bodies on which sporopollenin was deposited. Another important function of tapetal cells in pollen development process is the production of precursors for the synthesis of outer pollen wall (exine). During vacuolation of microspores, the tapetal cells undergo cell death and deposit cell remnants called tryphine or pollenkitt on the pollen surface. These substances function to protect the pollen grains from dehydration (Pacini et al. 1985, Bedinger, 1992).

In *B. distachyon*, the formation of intine (innermost layer of pollen wall) begins at vacuolated microspore stage and is completed by bicellular pollen stage of development. Bicellular pollen grains have distinct exine and intine walls. During bicellular and mature stages of pollen development, the intine stained pink-violet following PAS test (Fig. 5b, 6b), stained violet with toluidine blue (Fig. 5e, 6e) and gave weak reaction to protein test (Fig. 5d, 6d). Therefore, it was suggested that intine contains polysaccharides, pectin and a small amount of protein. From the bio-chemical aspect, intine is similar to the structure of primary cell wall of plants and thus composed of cellulosic and pectic contents (Goss 1968; Keijzer 1987; Bedinger 1992).

Prior to the first mitotic division, the uninucleate microspores become vacuolated and remain vacuolated in the bicellular stage. Our results are consistent with the earlier study in barley by Charzynska and Lenart (1989). Expansion of the vacuole is accompanied by the migration of the microspore nucleus and most of the cytoplasm to one end of the cell leaving a thin layer of cytoplasm around the vacuole itself (Fig. 4a, b). We found that, with the accumulation of starch in the bicellular pollen grain, the vacuole started diminishing gradually and disappeared completely before the second mitosis. Our results are consistent with earlier data on pollen development in rice (Zhang et al. 2011). Thus, starch accumulation started at the bicellular stage and continued until the mature pollen stage. Similar results have been reported in wheat (Mizelle et al. 1989). However, in sections of dehisced anthers (day 10) in *B. distachyon*, complete loss of starch granules was observed (Fig. 6f). Similar results showing hydrolysis of starch grains from one side of the pollen grain in dehisced anthers have been reported in rice by Raghavan (1988).

Morphological analysis showed that *B. distachyon* pollen grains are spheroidal in shape and contain a single pore with an operculum and annulus. This is in agreement with observations reported in other species of Poaceae (Chaturvedi et al. 1998; Nakamura et al. 2010). The

exine ornamentation pattern in *B. distachyon* is granular and in co-relation with rice (Zhang et al. 2011) and wheat (Goss 1968). The exine surface is continuous around the pollen grain except for the pore opening through which the pollen tube growth occurs during germination. This pore is spherical in shape similar to corn pollen (Goss 1968).

Acknowledgments

We thank Dr. Simon Crawford for technical guidance and access to Advanced Microscopy Facility, The University of Melbourne. Author; AS, also thanks Dr. Martin O'Brien for giving valuable suggestions. Financial support from the Australian Research Council (ARC DPO988972) is also gratefully acknowledged.

References

Alves SC, Worland B, Thole V, Snape JW, Bewan MW, Vain P (2009) A protocol for *Agrobacterium*-mediated transformation of *Brachypodium distachyon* community standard line Bd21. Nature Protocols 4:638-649

Bedinger P (1992) The remarkable biology of pollen. The Plant Cell 4:879-887

Charzynska M, Lenart N (1989) Pollen grain of barley (*Hordeum vulgare* L.) – pattern of development. Acta Soc Bot Pol 58(3):313-320

Chaturvedi M, Datta K, Nair PKK (1998) Pollen morphology of Oryza (Poaceae). Grana 37(2):79-86. doi: 10.1080/00173139809362647

Chen HN, Zhao CH, Liu XR (2012) Pollen development of *Cardiocrinum giganteum* (Wall.) Makina in China. Plant Syst Evol 298:1557-1565

Christensen JE, Horner HT, Jr, Lersten NR (1972) Pollen wall and tapetal orbicular wall development in *Sorghum bicolour* (Gramineae). Am J Bot 59:43-58

Draper J, Mur LA, Jenkins G, Ghosh-Biswas GC, Bablak P, Hasterok R, Routledge AP (2001) *Brachypodium distachyon*. A new model system for functional genomics in grasses. Plant physiol 127:1539-1555

El-Ghazaly G, Jensen WA (1986) Studies of the development of wheat (*Triticum aestivum*) pollen. I. Formation of the pollen grain wall. J Cell Sci 5:459-477

Eliseu SA, Dinis AM (2008) Ultrastructure and cytochemistry of *Eucalyptus globulus* (Myrtaceae) pollen grain. Grana 47(1):39-51

Garvin DF, Gu YQ, Hasterok R, Hazen SP, Jenkins G, Mockler TC, Mur LAJ, Vogel JP (2008) Development of genetic and genomic research resources for *Brachypodium distachyon*, a new model system for grass crop research. Crop Sci 48:S69-S84

Goss JA (1968) Development, physiology and biochemistry of corn and wheat pollen. Bot Rev 34:333-58

Halac ND, Cismondi IA, Rodriguez-Garcia MI, Fama G (2003) Distribution of pectins in the pollen apertures of Oenothera *hookeri.velans ster/+ster:*. Biocell 27(1):11-18

Heslop-Harrison J (1963) An ultrastructural study of pollen wall ontogeny in Silene Pendula. Grana Palynologica 4(1):7-24

Heslop-Harrison J, Dickinson HG (1969) Time Relationships of Sporopollenin Synthesis Associated with Tapetum and Microspores in *Lilium*. Planta 84:199-214

Heslop-Harrison J (1979) Aspects of the Structure, Cytochemistry and Germination of the Pollen of Rye (*Secale cereale* L.). Ann Bot 44:1-47

Hesse M (1986) Orbicules and the ektexine are homologous sporopollenin concretions in Spermatophyta. Plant Syst Evol 153:37-48

Hong SY, Park JH, Cho SH, Yang MS, Park CM (2011) Phenological growth stages of *Brachypodium distachyon*: codification and description. Weed Res doi: 10.1111/j.1365-3180.2011.00877.x

International *Brachypodium* Initiative (2010) Genome sequencing and analysis of the model grass *Brachypodium distachyon*. Nature 463:763-768

Itoh J, Nonomura K, Ikeda K, Yamaki S, Inukai Y, Yamagishi H, Kitano H, Nagato Y (2005) Rice plant development: from zygote to spikelet. Plant Cell Physiol 46:23-47

Keijzer CJ (1987) The process of anther dehiscence and pollen dispersal. II. The formation and the transfer mechanism of pollenkitt, cell wall development of the loculus tissues and the function of orbicules in pollen dispersal. New Phytol 105:499-500

Mizelle MB, Sethi R, Ashton ME, Jensen WA (1989) Development of the pollen grain and tapetum of wheat (*Triticum aestivum*) in untreated plants and plants treated with chemical hybridizing agent RH0007. Sex Plant Reprod 2:231-253

Nakamura AT, Longhi-Wagner HM, Scatena VL (2010) Anther and pollen development in some species of Poaceae (Poales). Braz J Biol 70(2):351-360

Opanowicz M, Vain P, Draper J, Parker D, Doonan JH (2008) *Brachypodium distachyon*: making hay with a wild grass. Trends Plant Sci 13:172-177

Pacini E, Franchi GG, Hesse M (1985) The Tapetum: Its Form, Function, and Possible Phylogeny in *Embryophyta*. Plant Syst Evol 149:155-185

Pigman W (2012) The Carbohydrates: Chemistry and Biochemistry, Edition 2. Elsevier

Raghavan V (1988) Anther and Pollen Development in Rice (Oryza sativa). Am J Bot 75:183-196

Rodriguez-Garcia MI, M'Rani-Alaoui M, Fernandez MC (2003) Behavior of storage lipids during development and germination of olive (*Olea europaea* L.) pollen. Protoplasma 221:237-244

Saini HS, Sedgley M, Aspinall D (1984) Developmental anatomy in wheat of male sterility induced by heat stress, water deficit or abscisic acid. Aust J Plant Physiol 11:243-53

Skvarla JJ, Larson DA (1966) Fine structural studies of Zea mays pollen. I. Cell membranes and exine ontogeny. Am J Bot 53:1112-1125

Steiglitz H (1977) Role of β-1,3-glucanase in postmeiotic microspore release. Dev Biol 57:87-97

Tütüncü Konyar S, Dane F (2012) Cytochemistry of pollen development in *Campis radicans* (L.) Seem. (Bignoniaceae). Plant Syst Evol 299(1):87-95

Tütüncü Konyar S, Dane F (2013a) Anther ontogeny in *Campis radicans* (L.) Seem. (Bignoniaceae). Plant Syst Evol 299(3):567-583

Tütüncü Konyar S, Dane F, Tütüncü S (2013b) Distribution of insoluble polysaccharides, neutral lipids and proteins in the developing anthers of *Campis radicans* (L.) Seem. (Bignoniaceae). Plant Syst Evol 299(4):743-760

Vain P (2011) *Brachypodium* as a model system for grass research. J Cereal Sci 54:1-7

Vithanage HIMV, Knox RB (1980) Periodicity of Pollen Development and Quantitative Cytochemistry of Exine and Intine Enzymes in the Grasses *Lolium perenne* L. and *Phalaris tuberosa* L. Ann Bot 45:131-141

Vogel J, Hill T (2008) High-efficiency *Agrobacterium*-mediated transformation of *Brachypodium distachyon* inbred line Bd21-3. Plant Cell Rep 27:471-478

Zhang D, Luo X, Lu Z (2011) Cytological analysis and genetic control of rice anther development. J Genet Genomics 38:379-390

Zhang D, Wilson ZA (2009) Stamen specification and anther development in rice. Chin Sci Bull 54:2342-2353

Table 1

Temporal developmental stages of anther and microspores of *B. distachyon*.

Days*	Plant material fixed and sectioned	No. of stages identified	Stages identified	Stage of the base floret
1	Spikelet	2	Archesporial cell stage, Primary parietal cell stage	Primary parietal cell stage
2	Spikelet	3	Primary sporogenous cell stage, Sporogenous cell stage and Pollen mother cell stage	Pollen mother cell stage
3	Spikelet	4	Primary parietal cell stage, Primary sporogenous cell stage, Sporogenous cell stage and Pollen mother cell stage	Pollen mother cell stage
4	Spikelet	3	Sporogenous cell stage, Pollen mother cell stage and tetrad stage	Tetrad Stage
5	Spikelet	3	Pollen mother cell stage, Tetrad stage and Free microspore stage	Free microspore stage
6	Anther	1	Vacuolated microspore stage	-
7	Anther	1	Vacuolated microspore stage	-
8	Anther	1	Bicellular pollen stage	-
9	Anther	1	Mature pollen stage	-

* Day 1: The first awn was just visible out of the flag leaf; Days 2-9: subsequent days after awn visibility; Day 9: anthesis, when yellow, mature anthers were clearly visible.

Table 2

Major cytological events during *B. distachyon* pollen development.

Stage	Anther Length* (mm)	Event
1) Pollen mother cell stage	< 0.3	Development of Microspore mother cells (MMCs), also called as Pollen mother cells (PMCs) occurs. Later, MMCs start meiotic division.
2) Tetrad stage	0.3-0.35	Formation of dyads and tetrads take place. At the end of first meiosis, one meiocyte forms two nuclei separated by cell plate. After meiosis II, tetrad containing four haploid microspores is formed enclosed in a callose wall.
3) Free microspore stage	0.4-0.45	Free haploid microspores, spherical in shape with thin exines are released from tetrads.
4) Vacuolated microspore stage	0.5-0.6	Microspores are irregularly shaped and become vacuolated, also known as uninucleate vacuolated microspores. Pore and exine formation in progress.
5) Bicellular pollen grain stage	0.65-0.75	Microspores undergo first mitotic division, generating a vegetative cell and a generative cell, known as bicellular pollen. Pollen grains began to accumulate starch.
6) Mature pollen grain stage	0.8-0.9	The generative cell undergoes second mitotic division and generates mature pollen grain containing three invisible nuclei. Mature pollen grains are completely filled with reserve substances.

* Florets were dissected and approximate length of anthers was measured with a binocular microscope.

Figure Legends

Fig. 1 *Brachypodium distachyon* at different stages of flowering. **a** *B. distachyon* plant at vegetative stage. **b** Immature spikelet at day 1, when awn is just visible (*arrow*). **c** Immature spikelet dissected at day 5. **d** Immature spike at day 7. **e** Mature, yellow anthers of *B. distachyon* in the base floret at day 9. Figures **a-d**, Bars, 1cm

Fig. 2 Light and fluorescent micrographs of semithin sections of spikelets at pollen mother cell stage of microsporogenesis. **a** Semithin section stained with DAPI. Nuclei are shown with *arrows*. **b** Toluidine blue staining of the anther at pollen mother cell stage. **c** Semithin section stained with Coomassie brilliant blue. **d** PAS staining showing absence of insoluble polysaccharides in the cytoplasm of pollen mother cells.

Fig. 3 Light and fluorescent micrographs of microspores at tetrad and free microspore stages of development. Semithin sections showing the formation of **a** dyads and **b** tetrads, stained with toluidine blue. **c** Coomassie brilliant blue staining at tetrad stage. **d** DAPI staining at tetrad stage. Microspore tetrads showing evident nuclei in their cytoplasm. **e** PAS staining at tetrad stage. **f** Semithin transverse section of anther free microspore stage of development, stained with toluidine blue (Dy, dyads; Tds, tetrads).

Fig. 4 Light and fluorescent micrographs of semithin longitudinal sections of anther at vacuolated microspore stage. **a** DAPI staining of vacuolated microspores showing nuclei at the periphery (*arrows*). **b** Vacuolated microspores stained with toluidine blue. Note the orientation of the developed pore towards tapetum (*arrows*). The black *asterisk* shows the same staining reaction of tapetum and microspore wall. **c** Coomassie brilliant blue staining showing weak reaction to for the presence of proteins in the cytoplasm of microspores. **d** PAS staining showing negative staining for insoluble polysaccharides. **e** Vacuolated microspores stained with Iodine-Potassium Iodide; note microspores showing negative staining for starch.

Fig. 5 Light and fluorescent micrographs of semithin anther sections at bicellular pollen stage. **a** DAPI staining showing vegetative (white *asterisk*) and generative (*arrow)* nuclei. **b** PAS staining; starch granules are shown by *arrows*. **c** Iodine-Potassium Iodide staining showing the presence of starch granules in the cytoplasm of bicellular pollen (*arrows*). **d** Semithin section stained with Coomassie brilliant blue. **e** Semithin section stained with toluidine blue. Bar, 50 µm

Fig. 6 Light and fluorescent micrographs of semithin anther sections at mature pollen stage. **a** DAPI staining showing trinucleate pollen (sperm nuclei are shown by *arrows* and vegetative nucleus is shown by white *asterisk*). **b** PAS staining showing abundance of starch granules in the cytoplasm of mature pollen (*arrows*). **c** Iodine-Potassium Iodide staining; note that starch granules (*arrows*) are abundant in cytoplasm. **d** Coomassie brilliant blue staining showing presence of proteins in the cytoplasm of mature pollen. **e** Semithin section stained with toluidine blue. **f** Semithin section of dehisced anther at day 10 stained with PAS; note the complete hydrolysis of starch grains.

Fig. 7 Pollen morphology under scanning electron microscope. **a** Mature anther of *B. distachyon* tweezed apart to release pollen grains. **b, c** Pollen grains covered with Ubisch bodies (*arrows*). **d** Magnified view of Ubisch bodies. **e, f** Mature pollen grain. The *arrow* indicates operculum and the black *asterisk* shows the annulus; note the granular pattern of pollen wall.

Fig. 1 *Brachypodium distachyon* at different stages of flowering. **a** *B. distachyon* plant at vegetative stage. **b** Immature spikelet at day 1, when awn is just visible (*arrow*). **c** Immature spikelet dissected at day 5. **d** Immature spike at day 7. **e** Mature, yellow anthers of *B. distachyon* in the base floret at day 9. Figures **a-d**, Bars, 1cm

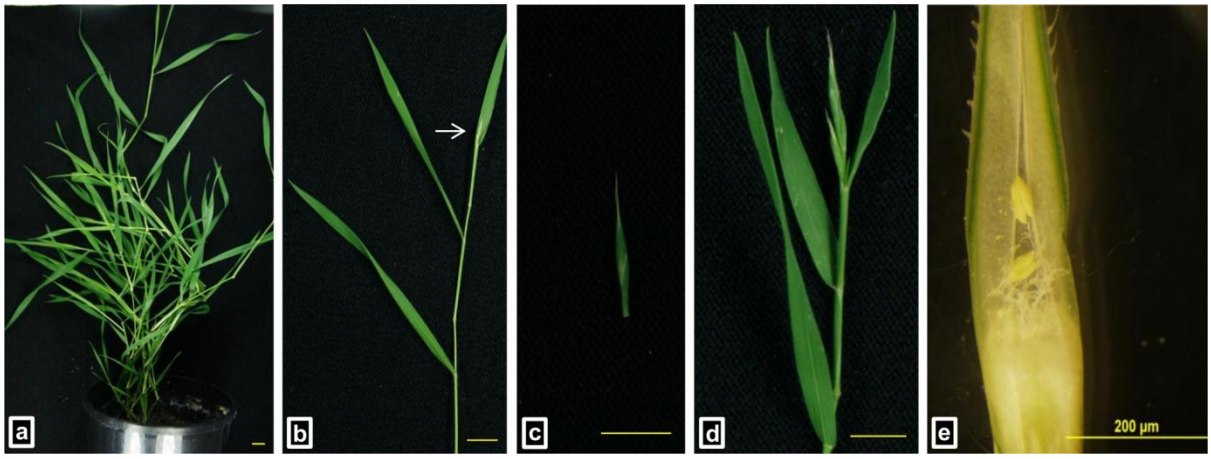

Fig. 2 Light and fluorescent micrographs of semithin sections of spikelets at pollen mother cell stage of microsporogenesis. **a** Semithin section stained with DAPI. Nuclei are shown with *arrows*. **b** Toluidine blue staining of the anther at pollen mother cell stage. **c** Semithin section stained with Coomassie brilliant blue. **d** PAS staining showing absence of insoluble polysaccharides in the cytoplasm of pollen mother cells.

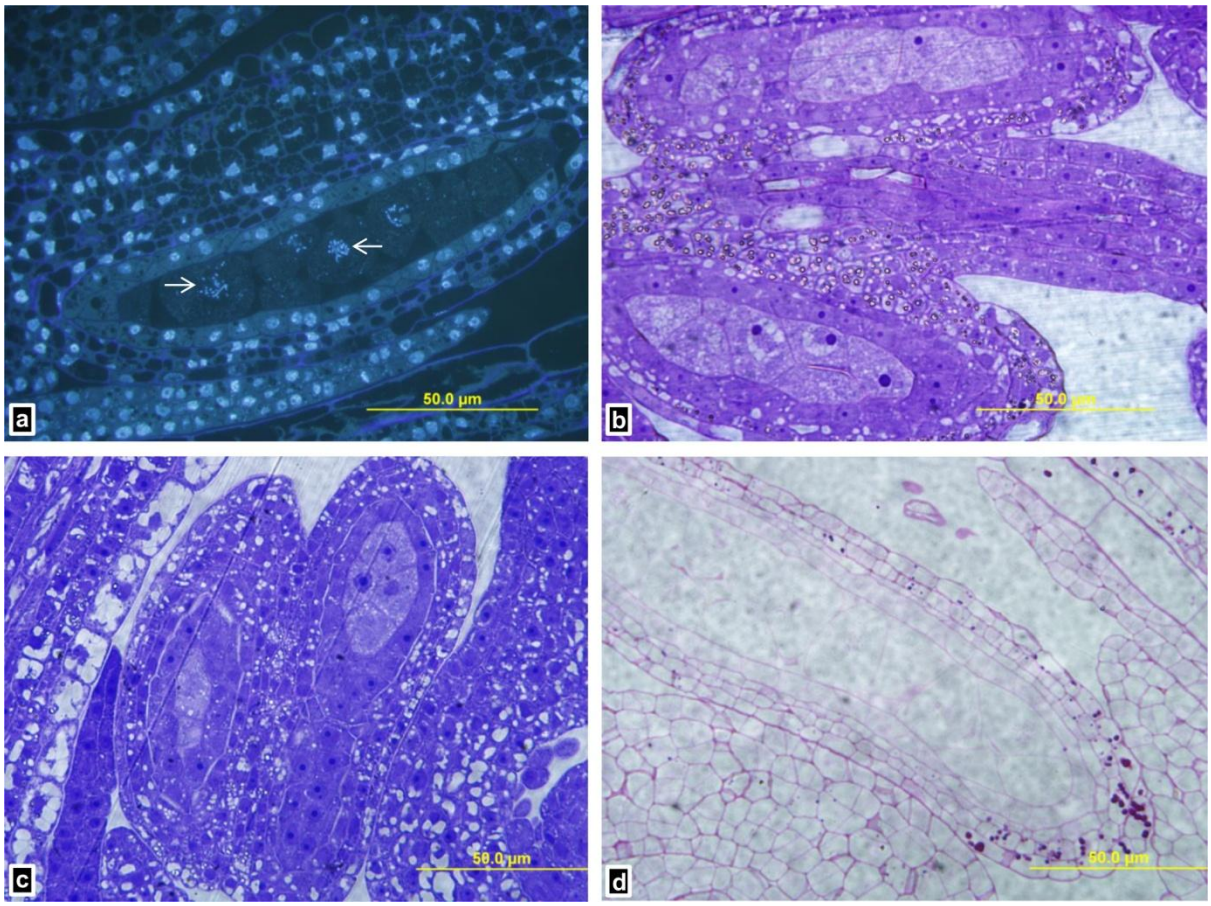

Fig. 3 Light and fluorescent micrographs of microspores at tetrad and free microspore stages of development. Semithin sections showing the formation of **a** dyads and **b** tetrads, stained with toluidine blue. **c** Coomassie brilliant blue staining at tetrad stage. **d** DAPI staining at tetrad stage. Microspore tetrads showing evident nuclei in their cytoplasm. **e** PAS staining at tetrad stage. **f** Semithin transverse section of anther free microspore stage of development, stained with toluidine blue (Dy, dyads; Tds, tetrads).

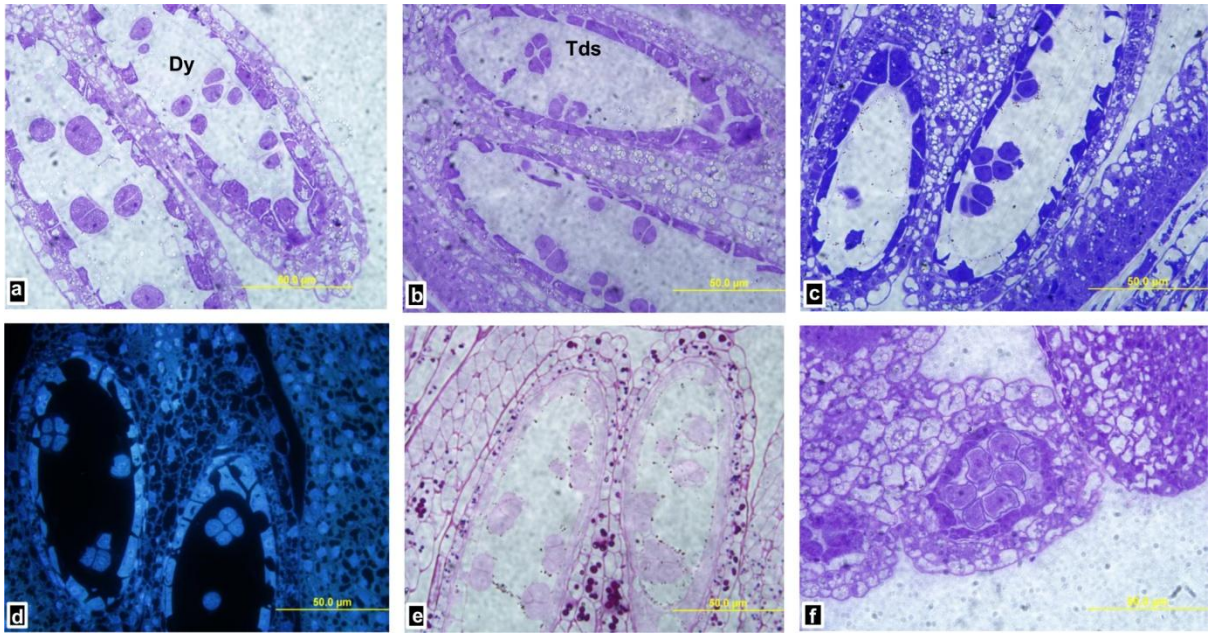

Fig. 4 Light and fluorescent micrographs of semithin longitudinal sections of anther at vacuolated microspore stage. **a** DAPI staining of vacuolated microspores showing nuclei at the periphery (*arrows*). **b** Vacuolated microspores stained with toluidine blue. Note the orientation of the developed pore towards tapetum (*arrows*). The black *asterisk* shows the same staining reaction of tapetum and microspore wall. **c** Coomassie brilliant blue staining showing weak reaction to for the presence of proteins in the cytoplasm of microspores. **d** PAS staining showing negative staining for insoluble polysaccharides. **e** Vacuolated microspores stained with Iodine-Potassium Iodide; note microspores showing negative staining for starch.

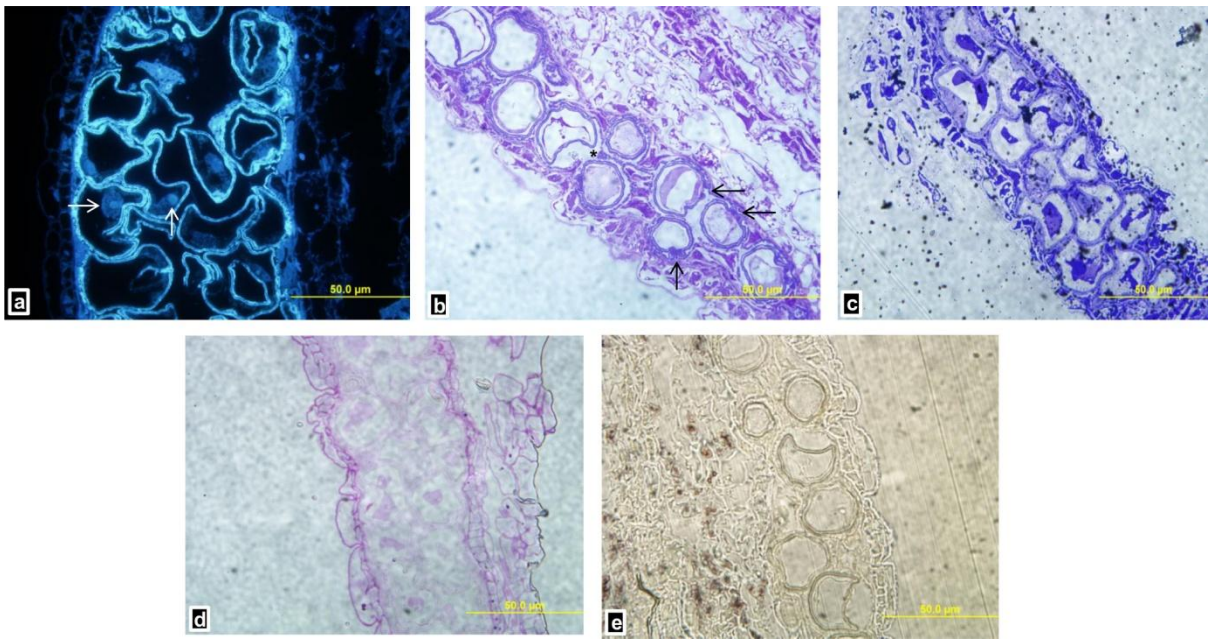

Fig. 5 Light and fluorescent micrographs of semithin anther sections at bicellular pollen stage. **a** DAPI staining showing vegetative (white *asterisk*) and generative (*arrow)* nuclei. **b** PAS staining; starch granules are shown by *arrows*. **c** Iodine-Potassium Iodide staining showing the presence of starch granules in the cytoplasm of bicellular pollen (*arrows*). **d** Semithin section stained with Coomassie brilliant blue. **e** Semithin section stained with toluidine blue. Bar, 50 µm

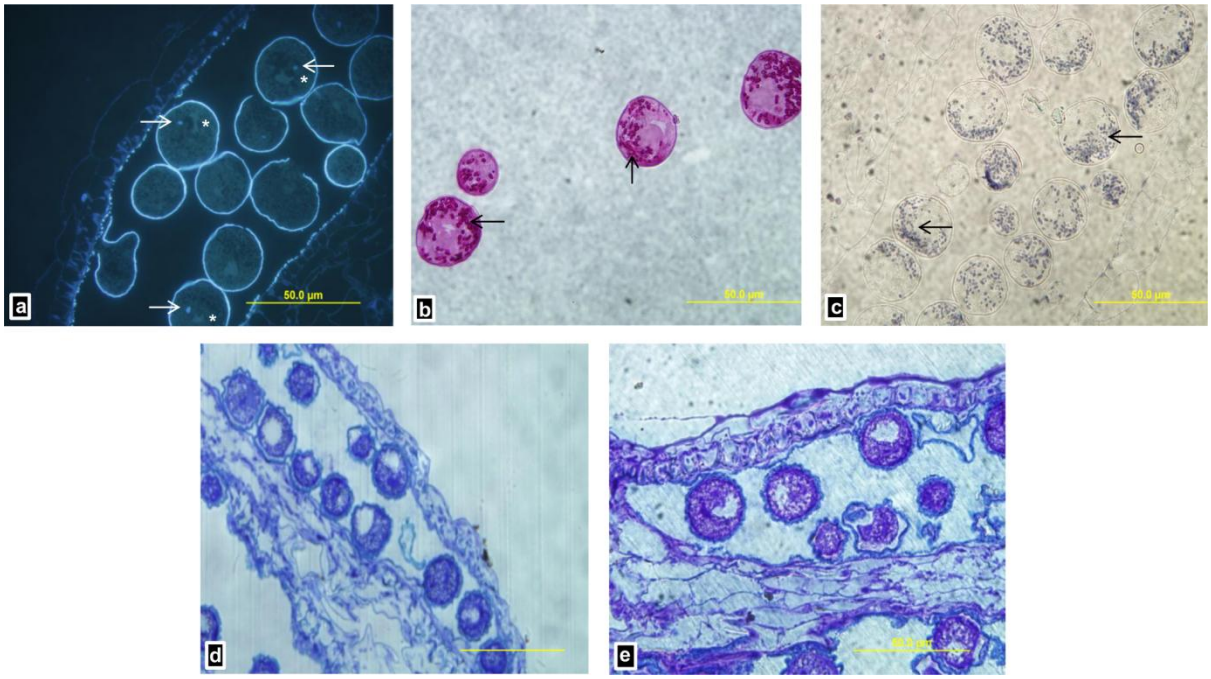

Fig. 6 Light and fluorescent micrographs of semithin anther sections at mature pollen stage. **a** DAPI staining showing trinucleate pollen (sperm nuclei are shown by *arrows* and vegetative nucleus is shown by white *asterisk*). **b** PAS staining showing abundance of starch granules in the cytoplasm of mature pollen (*arrows*). **c** Iodine-Potassium Iodide staining; note that starch granules (*arrows*) are abundant in cytoplasm. **d** Coomassie brilliant blue staining showing presence of proteins in the cytoplasm of mature pollen. **e** Semithin section stained with toluidine blue. **f** Semithin section of dehisced anther at day 10 stained with PAS; note the complete hydrolysis of starch grains.

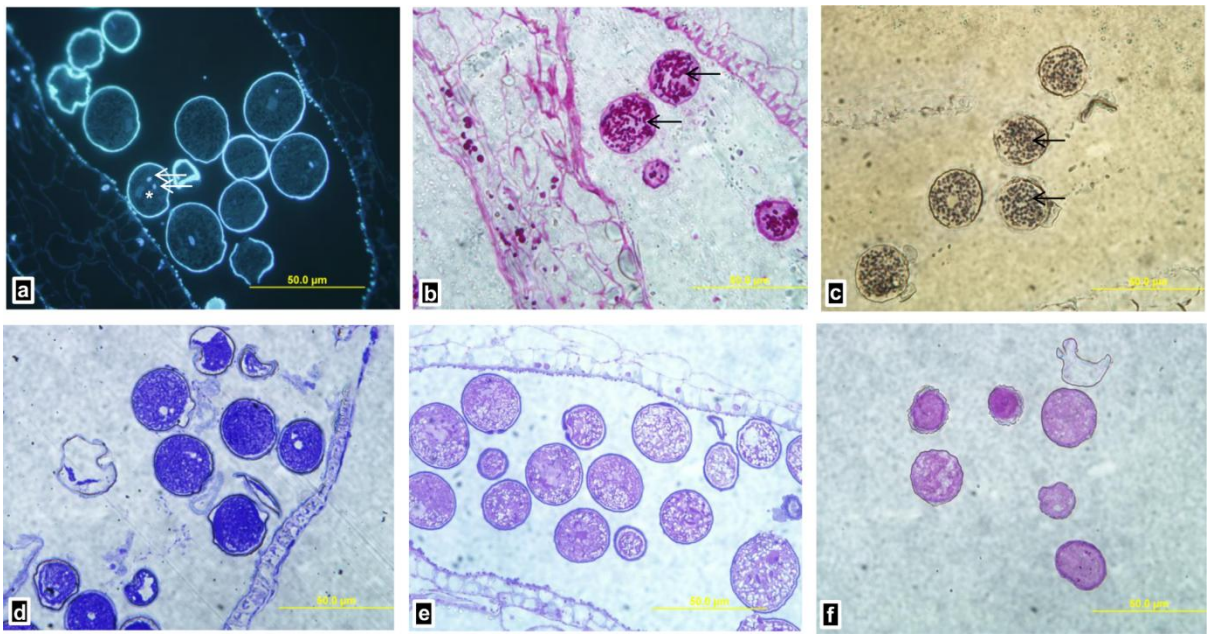

Fig. 7 Pollen morphology under scanning electron microscope. **a** Mature anther of *B. distachyon* tweezed apart to release pollen grains. **b, c** Pollen grains covered with Ubisch bodies (*arrows*). **d** Magnified view of Ubisch bodies. **e, f** Mature pollen grain. The *arrow* indicates operculum and the black *asterisk* shows the annulus; note the granular pattern of pollen wall.